Biomed Microdevices (2009) 11:313–322
DOI 10.1007/s10544-008-9237-9

Nanoscale patterning of kinesin motor proteins and its role in guiding microtubule motility

Vivek Verma · William O. Hancock · Jeffrey M. Catchmark

Published online: 7 November 2008

Abstract Biomolecular motor proteins have the potential to be used as 'nano-engines' for controlled bioseparations and powering nano- and microelectromechanical systems. In order to engineer such systems, biocompatible nanofabrication processes are needed. In this work, we demonstrate an electron beam nanolithography process for patterning kinesin motor proteins. This process was then used to fabricate discontinuous kinesin tracks to study the directionality of microtubule movement under the exclusive influence of surface bound patterned kinesin. Microtubules moved much farther than predicted from a model assuming infinite microtubule stiffness on tracks with discontinuities of 3 μm or less, consistent with a free-end searching mechanism. As the track discontinuities exceeded 3 μm, the measured and predicted propagation distances converged. Observations of partially fixed microtubules suggest that this behavior results from the interaction of the microtubules with the surface and is not governed predominately by the microtubule flexural rigidity.

Keywords Electron beam lithography · Kinesin patterning · Microtubule flexural rigidity

V. Verma
Department of Engineering Science and Mechanics,
Pennsylvania State University,
University Park, PA 16802, USA

W. O. Hancock
Bioengineering Department, Pennsylvania State University,
University Park, PA 16802, USA

J. M. Catchmark (✉)
Agricultural and Biological Engineering Department,
College of Agricultural Sciences, Pennsylvania State University,
109 Agricultural Engineering Building,
University Park, PA 16802, USA
e-mail: jcatchmark@engr.psu.edu

Present address:
J. M. Catchmark
Center for NanoCellulosics,
Pennsylvania Ben Franklin Technology Partners,
Center of Excellence, The Pennsylvania State University,
University Park, PA 16802, USA

1 Introduction

In eukaryotic cells, conventional kinesin (Howard 1996; Vale and Fletterick 1997; Warner and McIntosh 1999) motors transport intracellular cargo along microtubules, polymers of tubulin protein that measure 25 nm in diameter and several micrometers in length. Microtubules have a structural polarity, and kinesin motors move unidirectionally toward the plus- or fast-growing end of microtubules. Other biomotors such as dynein move towards the minus end of the microtubules, providing a two way transport system. Conventional kinesin has two heads, each measuring 4 nm×4 nm×7 nm, which use the energy from adenosine triphosphate (ATP) hydrolysis to walk in 8 nm steps along microtubules (Howard 1996; Kull et al. 1996; Coy et al. 1999). Individual kinesin motors can exert a maximal force of 6 pN (Svoboda et al. 1993) and work at efficiencies of ~50%. Kinesin motors can be immobilized on surfaces through their tail domain at densities of ~10^3 motors/μm^2 (Hancock and Howard 1998) and theoretically deliver cumulative forces in the range of nN/μm^2.

Developments in nanofabrication processes have enabled the synthesis of devices with nanometer scale dimensions (Yong Chen 2001; Craighead 2000; Christie and Donald 2003). The biomotor–microtubule system may be an ideal technology for powering and controlling the operation of such devices for drug delivery, biological assays or

molecular sorting. However, the creation of such hybrid devices requires nanoscale fabrication processes that are compatible with motor proteins, microtubules, and other associated support proteins such as casein. To this end, several fabrication approaches have been examined to position biomotors, align microtubules or direct the motion of microtubules propelled by immobilized biomotors. For example, Limberis et al. (2001) used fluid flow to align microtubules on a surface, and Brown et al. (2002) immobilized and extended microtubule seeds to produce a linear array of microtubules. To control the direction of microtubule transport, Hiratsuka et al. (2001) and Moorjani et al. (2003) used microscale lithography to create microchannels in photoresist on glass substrates. Cheng et al. (2005) used nanoimprinting of CYTOP on glass to achieve the same ends. These fabricated surfaces were then exposed to kinesin motors, and the resist channels were found to control the direction of microtubule transport. In all of these cases, the ability of the microchannels to guide the direction of microtubule transport relied upon the channel bottoms and sidewalls having different surface chemistries, such that functional motors were present only on the channel bottoms.

To date, approaches for selectively patterning kinesin motors have separated the microfabrication and surface engineering steps from the protein adsorption steps—generally heterogeneous surfaces are created and motors are exposed to the entire surface. One of the major reasons for not using lithography directly in protein patterning has been the perception that fabrication chemicals are lethal to proteins (Ilic and Craighead 2000). To address the incompatibility of proteins with lithography chemicals, we previously developed techniques for removing PMMA photoresist using chemicals that do not affect the functionality casein or kinesin motors (Verma et al. 2005).

2 Materials and methods

Electron beam lithography Electron beam lithography of poly methylmethacrylate (PMMA, Microchem) was used to pattern circular regions on glass cover slips (Corning, number 1 1/2, 22 mm^2). The process consisted of the following steps. Two percent PMMA 495 K was spin coated on several glass cover slips at 4,000 RPM for 40 s and then baked at 180°C for 2 min. A 200-Å thin film of gold was thermally evaporated onto the PMMA layer to conduct away the electrons during electron beam exposure. The gold film was etched away in Gold etch-type TFN (Transene Co. Inc., Danvers) after exposing the resist. The patterns were electron beam written at a dose of 825 μC/cm^2 using a Leica EBPG-5HR electron beam lithography system. Patterns were developed in 1:3 MIBK: IPA for 90 seconds and then rinsed in IPA for 1 min.

Microtubule motility assays Casein was prepared by dissolving casein powder in BRB80 buffer (80 mM PIPES, 1 mM $MgCl_2$, 1 mM EGTA, pH 6.9), centrifuging and filtering to remove insoluble components. A portion of the casein was labeled with Cy-5 dye following standard procedures (Amersham Biosciences, Buckinghamshire). Full-length *Drosophila* conventional kinesin was bacterially expressed and purified following standard procedures (Hancock and Howard 1998). For fluorescence studies, a mixture of 0.5 mg/ml unlabelled and 0.1 mg/ml Cy-5 labeled casein in BRB80 buffer was incubated in a flow cell containing the patterned PMMA cover slip for 5 min at room temperature. A motor solution consisting of 8.5 μg/ml kinesin motors, 0.2 mg/ml casein and 100 μM Mg-ATP in BRB80 buffer was then incubated in the flow cell for 10 min. To pattern the motors, the flow cell was disassembled by removing the tape, and the patterned cover slip was submerged in pure acetone bath for 30 min. To facilitate effective PMMA lift-off, a custom fixture was used to hold the glass cover slips during PMMA lift-off step, the acetone bath was rocked at 0.75 Hz, and the acetone was changed every 10 min. After PMMA removal step, another flow cell was made from the processed cover slip and the surface was imaged by either epifluorescence or total internal reflection microscopy (TIRF) using a Nikon TE2000 inverted microscope (60×, 1.45 NA, CFI Plan Apo TIRF oil objective).

Microtubules were polymerized bovine brain tubulin purified and rhodamine labeled according to standard procedures (Hyman 1991; Williams and Lee 1982). To polymerize microtubules, 4 mg/ml tubulin, 1 mM GTP, 4 mM $MgCl_2$ and 5% DMSO were combined in BRB80 buffer, and the temperature was raised to 37°C for 20 min. Polymerized microtubules were then diluted 40-fold in BRB80 containing 10 μM paclitaxel. After motors were patterned by PMMA removal, another flow cell was made from the acetone treated glass cover slip and motility solution (BRB80 with 20 mM D-glucose, 20 μg/ml glucose oxidase, 8 μg/ml catalase and 0.5% β-mercaptoethanol) containing 80 μg/ml rhodamine-labeled microtubules was introduced. Fluorescent microtubules were observed under epifluorescence microscopy (Nikon E600, 60×, 1.2 N. A. water immersion Plan Fluor objective).

3 Results

In the present work we demonstrate direct patterning of the motor protein kinesin and the associated support protein casein using electron beam lithography. Pattering is performed using a lift-off process employing the electron beam sensitive resist poly methyl methacrylate (PMMA).

By patterning PMMA on glass, adsorbing casein and kinesin to the surface, and then removing the PMMA, circular regions of motor proteins measuring as small as 250 nm in diameter can be directly patterned. This process exhibits several advantages including direct compatibility with standard fabrication techniques used to manufacture NEMS/MEMS devices, potential scalability to sub-20 nm dimensions, and the inherent ability to create a final planar surface in the unpatterned regions absent of chemical functionalization. These unpatterned regions can subsequently be functionalized with other biomotors or other relevant proteins to create new functional surfaces. This capability can be used, for example, to pattern two types of biomotors with opposite directionalities, presenting the possibility of bidirectionally controlled microtubule transport.

Electron beam lithography was used to create patterns of poly methylmethacrylate (PMMA, Microchem) on glass cover slips (Corning 1 1/2, 22 mm). Two patterns were examined: 3 μm diameter circles spaced 20 μm apart and 250-nm circles spaced 2 μm apart. Flow cells were constructed as shown in Fig. 1 using the PMMA patterned glass cover slips, and casein and kinesin were flowed into the chambers and allowed to adsorb to the patterned surface. The coverslip was then removed and immersed in acetone to remove the PMMA resist, leaving the glass substrate with motors patterned in defined regions. Surfaces were imaged by fluorescence microscopy to assess the effectiveness of the protein patterning and to verify that the kinesin motors remained functional after the patterning process.

Figure 2(a) depicts a fluorescence image of Cy-5 labeled casein and unlabeled kinesin patterned into circular regions measuring 3 μm in diameter and spaced at a distance of 20 μm. Fluorescence was observed in the patterned regions, indicating that the acetone wash did not remove the casein bound to the glass substrate. Furthermore, there was no measurable fluorescence from the regions previously covered with PMMA, indicating that the PMMA and the proteins adsorbed to it were removed, and that no redeposition of casein had occurred during the lift-off process.

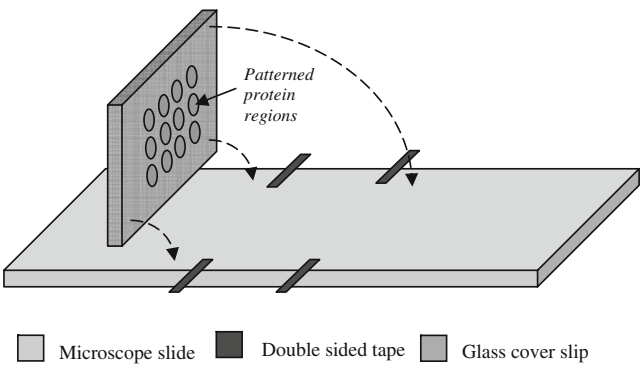

Fig. 1 Schematic of the flow cell used for performing motility assays. Tape was used only at the corners of the cover slip, which allowed the flow cell to be easily disassembled after protein incubation, enabling further processing of the glass cover slip

The effectiveness of kinesin patterning was first assessed using microtubule binding studies. Microtubules were sheared using a 30 gauge needle so that their lengths were comparable to the diameter of the patterned kinesin regions. Microtubules were then introduced into the flow cell for 20 min in the presence of 1 mM AMP-PNP (adenylylimidodiphosphate), a non-hydrolysable ATP analog that results in microtubules binding tightly to functional kinesin motors without moving. Cy-5 labeled casein and rhodamine labeled microtubules were imaged on the same processed sample using two different fluorescent filter sets. Figure 2(b) depicts fluorescence images showing that microtubules bound selectively to the regions where Cy-5 labeled casein and kinesin were patterned. This result indicates that there was no non-specific microtubule binding, and that the PMMA lift-off process produces highly specific patterning of kinesin and microtubules.

The scalability of this process to smaller patterned regions was also examined. Figure 3 depicts an array of 250 nm regions of patterned casein with a spacing of 2 μm. Electron beam lithography has the capability to directly pattern circular regions extending down to 20 nm (Vieu et al. 2000). When motors are adsorbed from solutions containing high kinesin concentrations, surface densities of 10^3 motors per square μm can be achieved (Hancock and Howard 1998), which corresponds to one motor in an area of roughly 30 nm×30 nm. Hence, this approach can potentially be used to specifically pattern individual kinesin motors on glass surfaces either by using small patterned regions or by using larger regions and lower motor concentrations.

To confirm that the functionality of the patterned kinesin motors was retained during the processing steps, microtubule gliding assays were performed on patterned motor samples. Using the PMMA lift-off process described in the experimental section, Cy-5 labeled casein and kinesin were patterned into 3 μm dots spaced 20 μm apart. When microtubules were introduced in the presence of 1 mM ATP, they were observed to bind and move only on those locations where fluorescence from Cy-5 labeled casein was present (Fig. 4). Microtubules moved at speeds of 586± 83 nm/s (N=30), confirming that motor patterning was specific and that the patterned motors are fully functional (Saxton et al. 1988).

4 Discussion

An important application of biomotor patterning is to create tracks of proteins that guide the motion of microtubules.

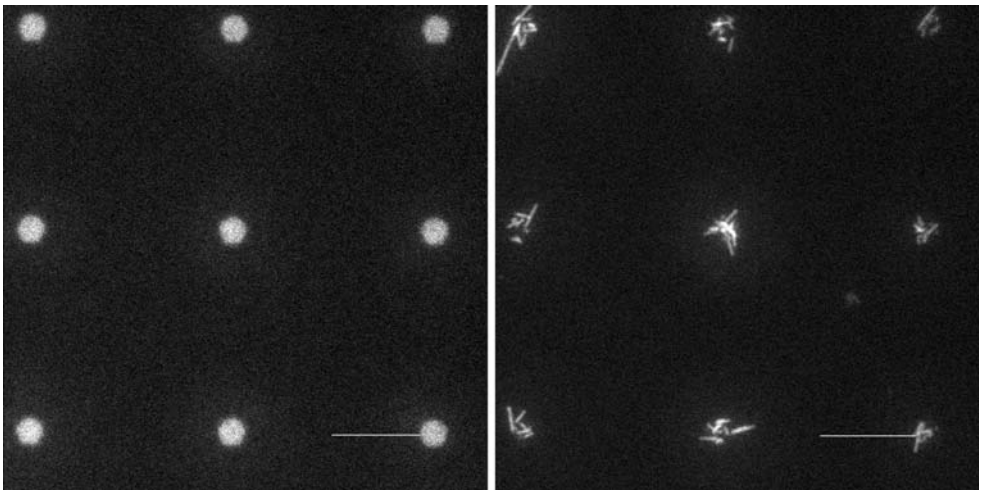

Fig. 2 (**a**) Fluorescence images of 3 μm diameter circular regions of Cy-5 labeled casein and kinesin motors patterned using the PMMA electron beam lithography lift-off process and spaced at 20 μm intervals. No binding in the unpatterned region of casein was observed. (**b**) Fluorescence image of rhodamine-labeled microtubules incubated with the patterned motor sample in 1 mM AMP-PNP. Microtubules bound specifically to the patterned kinesin motors, and binding of microtubules in the unpatterned region was not observed. *Scale bar* is 10 μm

(a) **(b)**

Controlling the direction of microtubule propagation could enable several applications including molecular sorting and the development of new lab-on-a-chip devices where microtubules carry cargo against fluid flow or concentration gradients. Reuther et al. (2006) recently showed that microtubules can be effectively used as templates to pattern linear tracks of motors on surfaces, but the pattern lengths are limited by the lengths of the microtubule templates used, and because the microtubules land randomly on the surface it is difficult to control the location of the motor tracks. Because electron beam lithography can be used to precisely generate virtually any desired pattern, this approach was implemented to fabricate discontinuous tracks of kinesin motors. The hypothesis is that by creating specific patterns of motors on surfaces, the direction of microtubule transport can be controlled to maximize the distance of transport in selected directions. Microtubule propagation on such small features has not been examined to date.

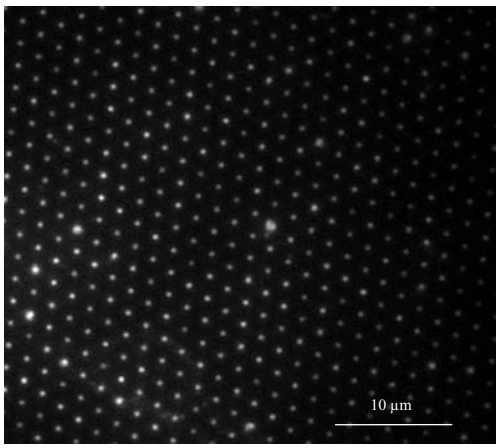

Fig. 3 Fluorescence image of 250 nm diameter Cy-5 labeled casein dots patterned using PMMA lift-off and spaced at 2-μm intervals. *Scale bar* is 10 μm

Due to their relatively high stiffness, microtubules generally move across kinesin-functionalized surfaces in relatively straight lines. However, in regions sparsely decorated with motors, the leading end of a moving microtubule undergoes thermal fluctuations that increase the area over which it "searches" for new motors. Previous studies on the impact of surface-patterned biomotors on microtubule directionality have predicted a minimum microtubule radius of curvature $r=\pi EI/4k_BT$ where E is the modulus and I is the geometric moment, k_B is Boltzmann's constant and T is temperature (Gittes et al. 1993; Hess et al. 2002; Hunt and Howard et al. 1993). Using a number of different experimental procedures, measured values of EI for microtubules range from 2×10^{-24} Nm^2 (Kikumoto et al. 2006) to 2.2×10^{-23} Nm^2 (Gittes et al. 1993). These values translate into radii of curvature, r, ranging from 382 to 4200 μm. This approach implies that microtubules traveling along patterned tracks of motors would need to remain almost perfectly parallel to the track or else they would run off of the track (Hess et al. 2002).

To explore the behavior of microtubules on precisely patterned regions of functional motors, microtubule motility was examined on a novel geometry consisting of linear arrays of circular protein patterns measuring 3 μm in diameter and spaced 3, 6, 9, and 12 μm center-to-center (where the 3 μm spacing results in a continuous linear track being formed). The propagation characteristics were examined for 47 microtubules ranging in length from 4.3 μm, which is comparable to the size of the patterned protein regions and is much less than the largest separation of 9 μm, to 43.4 μm, which is over four times the largest separation distance. The arrays were separated by 25 μm as shown in Fig. 5. To create patterns of functional motors, photoresist was patterned onto glass coverslips using electron beam lithograph, casein and kinesin were then adsorbed to the surface and the photoresist was removed,

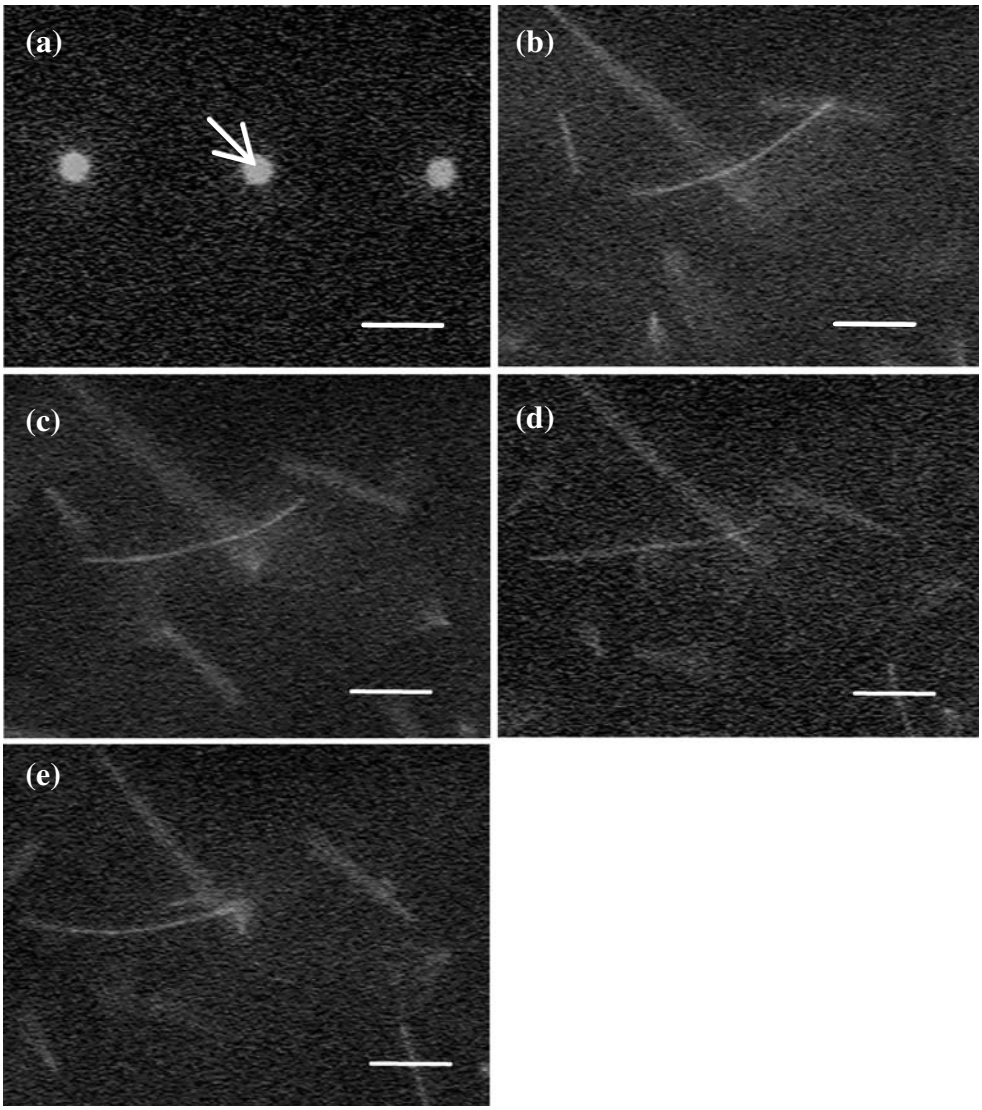

Fig. 4 Fluorescence images of microtubule movement on lithographically patterned kinesin regions (*arrow*). (**a**) Image showing the florescence of three 3 μm diameter regions of Cy-5 labeled casein and functional kinesin. (**b**)–(**e**) Images of rhodamine-labeled microtubules at t=0, 7, 14, and 21 s, respectively. Microtubules were observed to bind and move only on the regions where fluorescence from Cy-5 casein was present. *Scale bar* is 10 μm

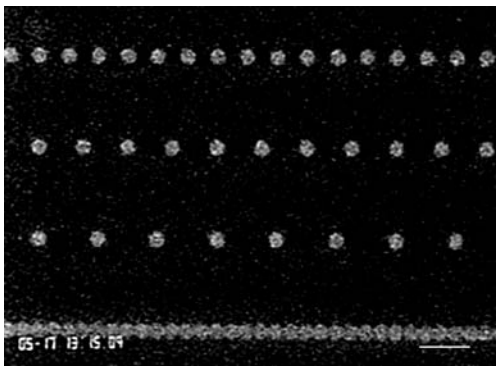

Fig. 5 Fluorescence image of four linear arrays of 3-μm diameter dots of Cy-5 labeled casein and functional kinesin motors patterned using PMMA lithography. Dot spacing is 3 μm, 6 μm, 9 μm and 12 μm (center to center). *Scale bar* is 10 μm

and flow cells were assembled as described above. Microtubules were introduced into the flow cell and the motility dynamics were assessed. Specifically, the total length of propagation of all microtubules that initially spanned two or more circular patterned regions was measured and the actual microtubule propagation length was calculated by subtracting the microtubule length from the total measured propagation length. This length adjustment was used to eliminate variations associated with the wide variation of microtubule lengths.

Assuming that the initial orientation of the microtubules is random and that the modulus of the microtubule is infinite, i.e., the patterned kinesin can not impact the direction of microtubule propagation, the percentage of microtubules that continue to propagate a distance l along the fabricated protein tracks can be estimated from a simple geometric model. Microtubules that span two adjacent patterned regions can take on a range of initial angles relative to the axis of the patterned motor track (θ_i), while

microtubules that are captured by a patterned region at a distance l represent a smaller range of angles (θ_c). We have assumed in the model that the microtubule passes through center of the patterned region. The probability that a microtubule will propagate a distance l is the ratio of these angles, given by:

$$P_{mt}(l) \cong \frac{\theta_c}{\theta_i} = \arctan\left(\frac{w}{2(l+d)}\right) \Big/ \arctan\left(\frac{w}{2d}\right) \quad (1)$$

where l is the microtubule propagation length, w is the diameter of the circular kinesin-patterned regions, and d is center to center spacing of the patterned regions. This model is illustrated in Fig. 6.

To explore this behavior, the directionality of 47 microtubules exhibiting a wide distribution of microtubule lengths relative to the size and discontinuity spacing of the biomotor tracks was examined. The percentage of microtubules continuing to propagate on the patterned tracks was compared to that predicted by a statistical model assuming infinite flexural modulus of microtubule. In Fig. 7(a–b), the predicted and measured propagation distances are plotted for discontinuities ranging from 3 to 12 μm. For propagation distances less than 50 μm, the percentage of microtubules that continue to propagate far exceeds the predictions from the model. In the cases where d=3 or 6 μm, the measured percentages exceed the predicted percentages by as much as a factor of four. The measured percentages begin to converge with the predicted percentages for propagation lengths greater than 60 μm, and as d is increased to 12 μm.

To understand this behavior more thoroughly, we studied the dynamics of two microtubules whose ends were fixed to motor-patterned regions, resulting in free ends measuring 23 and 16 μm, respectively. The microtubules were fixed to patterned kinesin using adenosine diphosphate (ADP). ADP is non-hydrolysable analog of adenosine triphosphate which helps to lock microtubules to kinesin motors. The free ends of the microtubules were located in the region where the surface was blocked with casein and the ends did not appear to interact with the surface. The bend angle was measured as the deviation of the leading end of microtubule

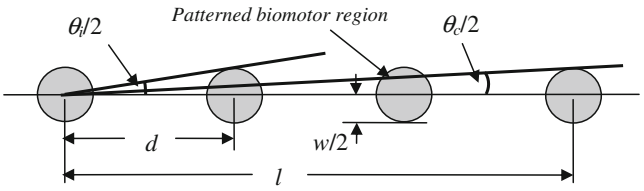

Fig. 6 Geometry used to calculate the probability that microtubules propagate a distance l assuming an infinite elastic modulus. The probability $P_{mt}(l) \cong \theta_c/\theta_i$ where θ_c=arctan ($w/2(l+d)$), θ_c=arctan ($w/2d$), w is the radius of the patterned kinesin regions, and d is the center-to-center distance

from the portions of microtubule that was fixed. An extended line was drawn between the fixed ends of microtubule and was treated as the reference line. Another line joining the last bound point of microtubule on the dot and the leading tip was drawn. The angle between these two lines was measured as the bend angle. Figure 8(a–b) depicts a plot of fluctuations in the microtubule bend angle over time. The bend angle is defined as the angle between a line drawn parallel to the fixed region of the microtubule end and a line drawn between the proximal end of the fixed region and the free tip of the microtubule. The deviation of the free tip was calculated by multiplying length of free end of microtubule by the sine of the measured angle. This process was repeated 50 times for both microtubules. The insets of the figures contain photographs of the microtubules indicating where they were fixed at one end. During the time interval shown, the observed microtubule did not interact with any other microtubule. The maximum angular deviation from the normal position of these microtubules is ~4° for the long microtubule (Fig. 8(a)) and 5.4° for the shorter microtubule (Fig. 8(b)). It is possible to estimate the flexural rigidity EI of a cylindrical beam by tracking thermally driven fluctuations in the free end over time and using the equation (Cassimeris et al. 2001):

$$\mathrm{EI} = \frac{k_B T L^3}{3\langle y^2 \rangle} \quad (2)$$

Here, L is the length of the free end of the microtubule and $\langle y^2 \rangle$ is the mean square displacement of the microtubule tip. For the fixed microtubules shown in Fig. 8(a and b), the EI was calculated to be 4.3×10^{-23} Nm^2 and 1.3×10^{-23} Nm^2, respectively. These values of EI are in the range of previous measurements—they are in agreement with values from Gittes et al (1993), but are higher than values reported by Kikumoto et al. (2006). Moreover, using an average EI value of 2.8×10^{-23} Nm^2, a minimum microtubule radius of curvature r=5,300 μm is calculated, consistent with values calculated by Hess et al. (2002).

The predicted bend radius based on the angle measurements from immobilized microtubules suggests that the microtubule rigidity prevents patterned motors from guiding microtubule propagation. However, the results shown in Fig. 7(a) suggest that microtubules are preferentially directed to the next patterned region by the patterned kinesin. To better understand this, movies from three microtubules moving over the patterned motors were carefully analyzed. Two of these microtubules, measuring 13.0, and 23.5 μm in length, moved along patterned kinesin tracks with a 3 μm pitch, and the third microtubule, which measured 8.5 μm in length, moved along a track with a 6 μm pitch. Images taken from these videos, depicting the redirection of microtubule propagation, are shown in

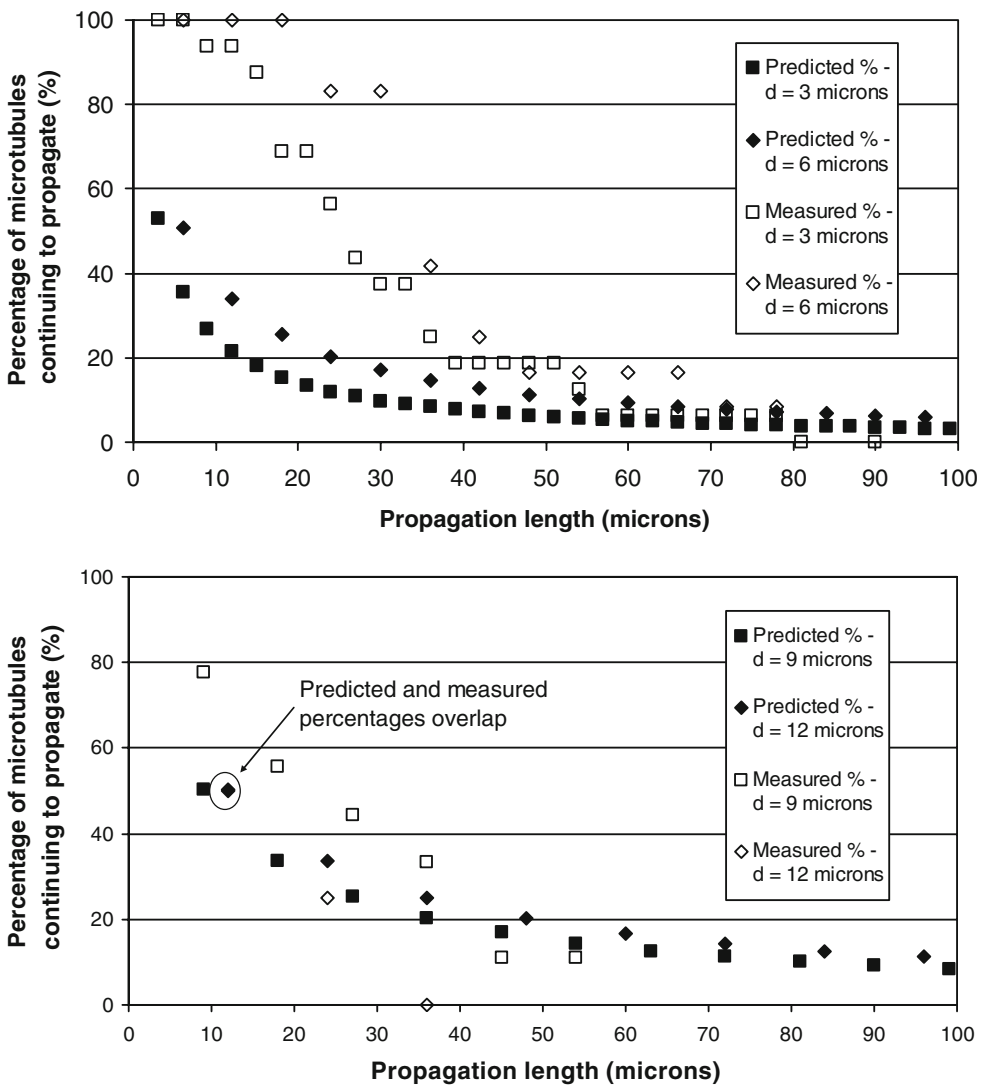

Fig. 7 Plot of the predicted and measured propagation distances for motors patterned in 3-μm circles with center to center spacing, *d*, of (**a**) 3 and 6 μm, and (**b**) 9 and 12 μm. For *d*=3 and 6 μm the actual run length of microtubules exceed the predicted behavior, demonstrating successful directional guiding by surface patterned kinesin dots

Fig. 9(a–c). For each of these microtubules, the leading end propagates off of the patterned kinesin region and begins a thermally driven searching motion. The free end then binds to a motor on an adjacent patterned region, and is redirected back onto the kinesin track. None of the microtubules observed interacted with other microtubules during the redirection process. The maximum measured deflection angle was 8°, 10°, and 15° for the microtubules measuring 8.5, 13.0 and 23.5 μm, respectively. These values are higher than those measured for the immobilized microtubules shown in Fig. 8(a–b), despite the fact that the observation times where somewhat shorter. It is unclear why these microtubules exhibited an apparently lower flexural rigidity. Possible explanations include a spatially localized reduction in modulus based on defects in the microtubule structure (VanBuren et al. 2005; Boal et al. 2006) or possibly a bending of the filament from the active kinesin motors interacting with the microtubule.

Lateral fluctuations in the microtubule leading end is only one determinant of the interaction between microtubules and surface bound motors. Another issue is the probability that the free end of the microtubule will be sufficiently close to motor for binding. For neighboring motors to redirect the motion of a microtubule, the microtubule must come into close proximity to the surface (~80 nm or less depending upon the length of the kinesin tail and the location of the kinesin head relative to the surface) for an interval of time that allows the motors to bind to the filament. It is expected that for a microtubule being guided along patterned motor regions with small center-to-center spacing, the short length of the microtubule free end will ensure that it remains close to the surface. However, with increased spacing distances, the microtubule free ends are expected to undergo larger magnitude fluctuations, and hence may spend a significant fraction of the time away from the surface. To study this phenomenon,

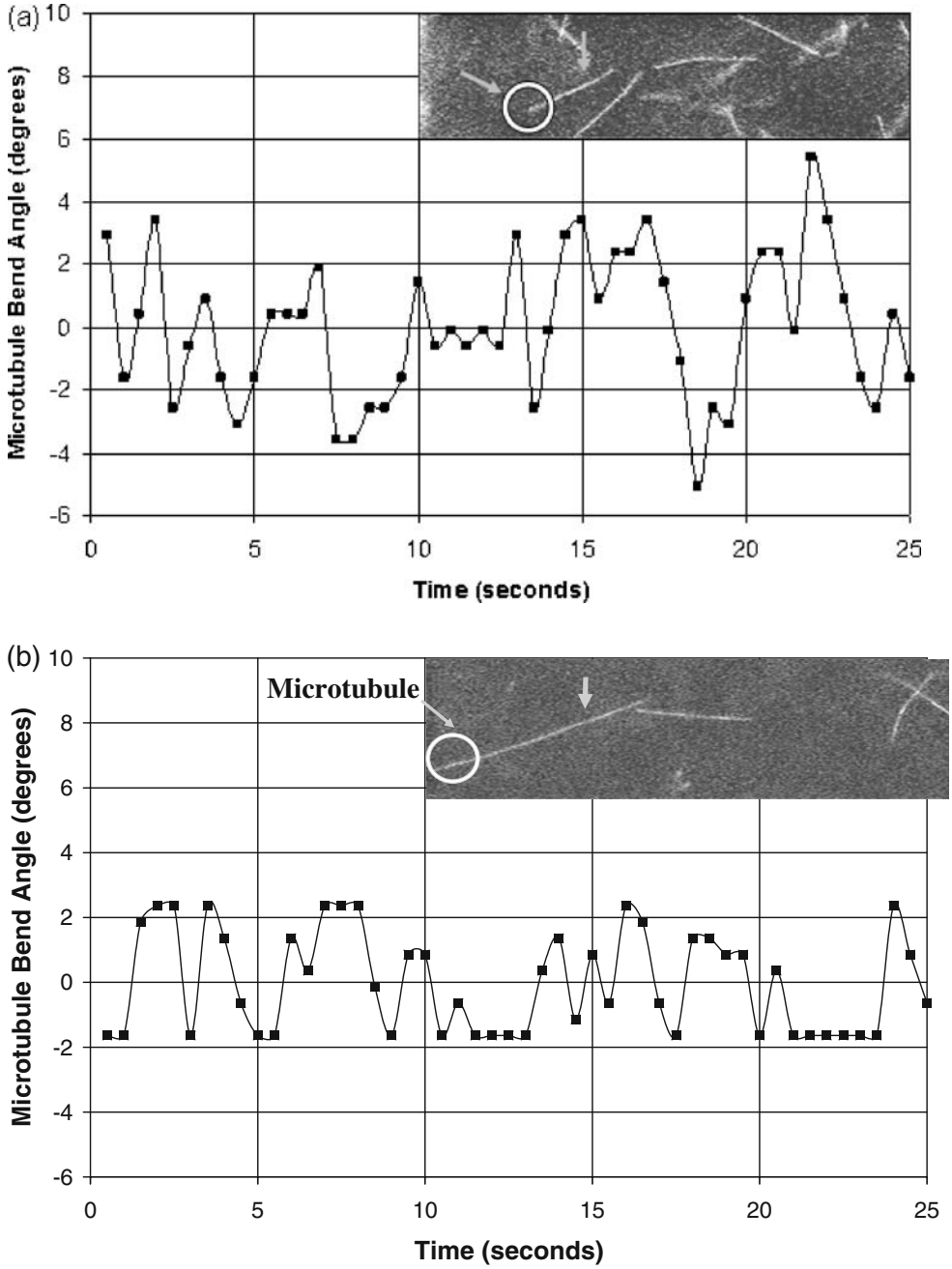

Fig. 8 Plot of the measured bend angle over time for microtubules fixed on one end. Data were taken during a time interval in which no other microtubules interacted with the fixed microtubule. *Inset*: still photograph of the rhodamine-labeled microtubule. The *white vertical arrow* indicates where the microtubule was fixed to the surface. The lengths of the microtubules free ends were (**a**) 16 μm and (**b**) 21 μm

we used the same microtubules shown in Fig. 8(a–b), to qualitatively assess the position of the microtubule with respect to the surface as a function of time. Microtubules were imaged with a Nikon E600 (60× objective, 1.2 N.A.) which exhibits a depth of focus of ~500 nm. It was recently shown that in a geometry similar to ours that kinesin motors elevate microtubules less than 20 nm above the glass surface (Kerssemakers et al. 2006), so if the objective is focused on the glass surface, then microtubule segments ~250 nm from the surface or less will appear crisp, while segments farther away from the surface will appear out of focus. Over 100 still images of the microtubules were examined. It was found that ~70% of the time the free microtubule end is positioned away from the surface, including a 20-s continuous interval. If this microtubule were not immobilized, it would have propagated ~20 μm over this interval before returning to the surface. Furthermore, this is also an overestimate of the time spent within

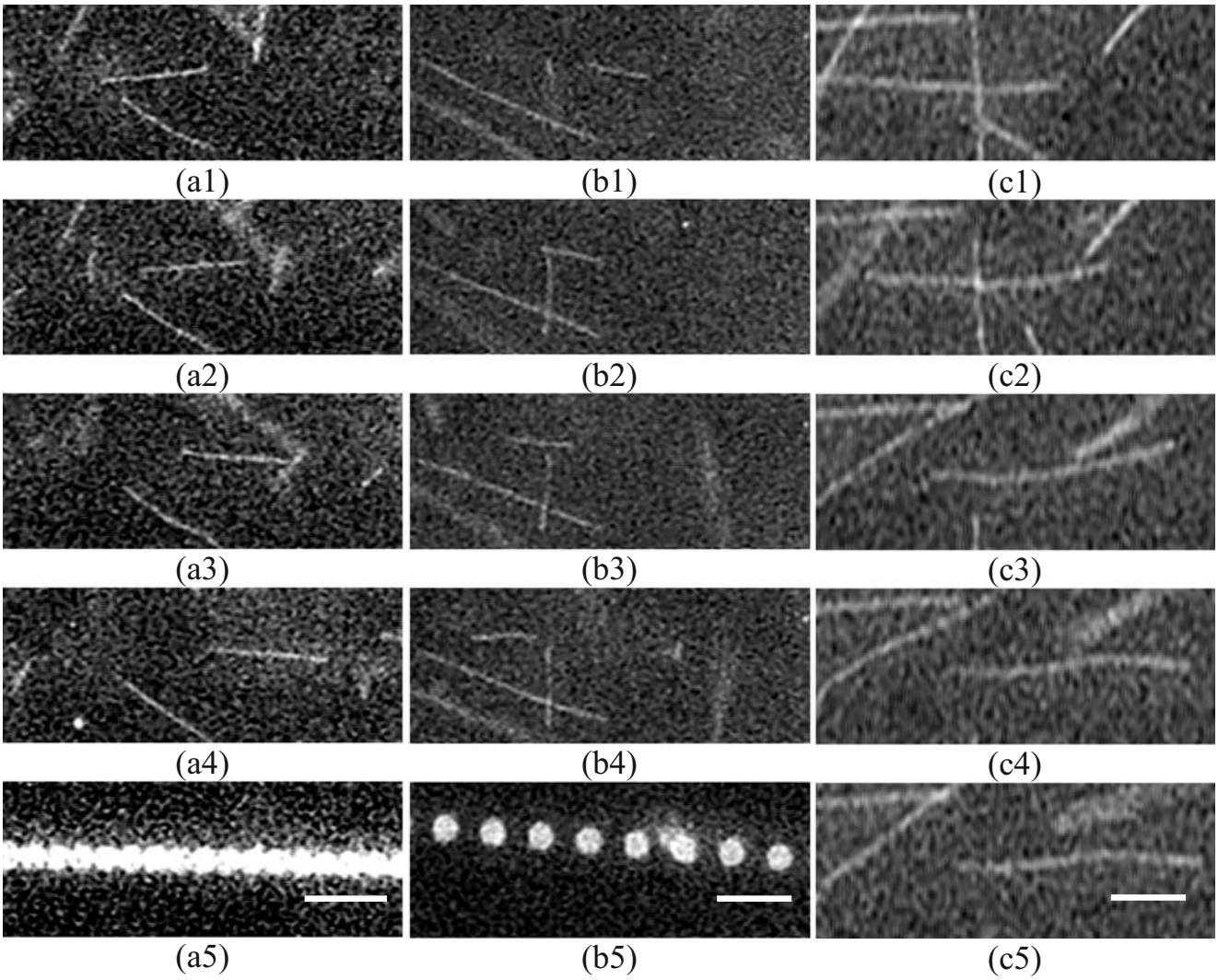

Fig. 9 Images of microtubule movement showing microtubule guiding by the patterned kinesin dots. In each case, the leading end of the microtubule was observed to search over an area of the surface and bind to the next available kinesin dot. Images (*a1*)–(*a4*) were taken at t=0, 3.5, 7, and 10.5 s, respectively. Images (*b1*)–(*b4*) were taken at t=0, 5, 9, and 13 s, respectively. Images (*c1*)–(*c5*) were taken at t=0, 3, 8.1, 9.1, and 10.1 s, respectively. All *scale bars* are 10 μm

<80 nm of the surface (the contour length, and hence the expected maximal reach of conventional kinesin; Howard 1996), since our qualitative assessment of the position of the microtubule while near the surface is only accurate to within ~250 nm. Hence, although the microtubule flexural rigidity allows the free end to search over a relatively wide area, thermal fluctuations of the filament tip normal to the surface decrease the probability that the microtubule will bind to motors immobilized on the surface. In addition, it can't be ruled out microtubules also have small degrees of curvature that cause the leading end to bend away from the surface. This microtubule curvature has been noted by others (Gittes et al. 1993; Amos and Cross 1997).

In conclusion, the present study demonstrates that functional kinesin motor proteins can be patterned through electron beam lithography and a PMMA lift-off process that is compatible with standard MEMS/NEMS fabrication processes. Protein-containing regions as small 250 nm were patterned on glass substrates with no measurable non-specific binding. Surprisingly, kinesin motors retain their microtubule transport function, demonstrating the biocompatibility of this process with this type of biomotor protein. The use of such conventional nanoscale patterning approaches, which directly integrate biological molecular motors and associated proteins, provides a new capability for engineering new hybrid synthetic and biological devices and systems.

This novel biomotor patterning process was used to investigate the directionality of microtubule propagation on discontinuous kinesin tracks. The percentage of microtubules propagating long distances along the patterned tracks was compared to that predicted by a statistical model

based on the track geometry and assuming infinite elastic modulus of the microtubule. Interestingly, on tracks exhibiting no discontinuity or a discontinuity of 3 μm, microtubules traveled much farther than predicted from the statistical model. From observing the microtubule behavior, it is clear that thermal fluctuations in the leading end enables the filaments to interact with subsequent patterned regions, resulting in a change in the propagation direction and continued motion along the patterned track. In contrast, for discontinuities of 6 or 9 μm and for distances exceeding 60 μm, the propagation distances begin to converge with the model predictions. Qualitative studies of the leading microtubule end indicated that the leading segment remains within a few hundred nanometers of the surface approximately one third of the time. It is hypothesized that the relatively fast microtubule transport velocity in conjunction with the small percentage of time the free microtubule end spends in close proximity to the surface is responsible for the inability of patterned motors to guide microtubules indefinitely. These results put an upper limit on the optimal motor spacing that best enables long distance transport on kinesin-patterned surfaces.

Acknowledgements This work was supported by The Pennsylvania State University Center for Nanoscale Science, a NSF Materials Research Science and Engineering Center (DMR0213623). It was also supported by the National Nanotechnology Infrastructure Network (NSF Cooperative Agreement No. 0335765 with Cornell University) and The Pennsylvania State University Materials Research Institute. V. V wishes to thank the Haythornthwaite Foundation for their Founder's Prize and grant for year 2005–06.

We thank Maruti Uppalapati for purifying kinesin and Gayatri Muthukrishnan for purifying and labeling tubulin. We also thank Dr. Edward Basgall and Dr. Khalid Eid for assistance with electron beam lithography.

References

L.A. Amos, R.A. Cross, Curr. Opin. Struct. Biol. **7**, 239 (1997) doi:10.1016/S0959-440X(97)80032-2

A.K. Boal, H. Tellez, S.B. Rivera, N.E. Miller, G.D. Bachand, B.C. Bunker, Small **2**, 793 (2006) doi:10.1002/smll.200500381

T.B. Brown, W.O. Hancock, Nano Lett. **2**, 1131 (2002) doi:10.1021/nl025636y

L. Cassimeris, D. Gard, P.T. Tran, H.P. Erickson, J. Cell Sci. **114**, 3025 (2001)

L.-J. Cheng, M.-T. Kao, E. Meyhöfer, L.J. Guo, Small **1**, 409 (2005) doi:10.1002/smll.200400109

R.K.M. Christie, M.T. Donald, J. Vac. Sci. Technol. A **21**, S207 (2003) doi:10.1116/1.1600446

D.L. Coy, M. Wagenbach, J. Howard, J. Biol. Chem. **274**, 3667 (1999) doi:10.1074/jbc.274.6.3667

H.G. Craighead, Science **290**, 1532 (2000) doi:10.1126/science.290.5496.1532

F. Gittes, B. Mickey, J. Nettleton, J. Howard, J. Cell Biol. **120**, 923 (1993) doi:10.1083/jcb.120.4.923

W.O. Hancock, J. Howard, J. Cell Biol. **140**, 1395 (1998) doi:10.1083/jcb.140.6.1395

H. Hess, J. Clemmens, C.M. Matzke, G.D. Bachand, B.C. Bunker, V. Vogel, Appl. Phys., A Mater. Sci. Process. **75**, 309 (2002) doi:10.1007/s003390201339

Y. Hiratsuka, T. Tada, K. Oiwa, T. Kanayama, T.Q. Uyeda, Biophys. J. **81**, 1555 (2001)

J. Howard, Annu. Rev. Physiol **58**, 703 (1996) doi:10.1146/annurev.ph.58.030196.003415

A.J. Hunt, J. Howard, Proc. Natl. Acad. Sci. USA **90**, 11653 (1993) doi:10.1073/pnas.90.24.11653

A.A. Hyman, J. Cell Sci. Suppl. **14**, 125 (1991)

B. Ilic, H.G. Craighead, Biomed. Microdevices **2**, 317 (2000) doi:10.1023/A:1009911407093

J. Kerssemakers, J. Howard, H. Hess, S. Diez, Proc. Natl. Acad. Sci. USA **103**, 15812 (2006) doi:10.1073/pnas.0510400103

M. Kikumoto, M. Kurachi, V. Tosa, H. Tashiro, Biophys. J. **90**, 1687 (2006) doi:10.1529/biophysj.104.055483

F.J. Kull, E.P. Sablin, R. Lau, R.J. Fletterick, R.D. Vale, Nature **380**, 550 (1996) doi:10.1038/380550a0

L. Limberis, J.J. Magda, R.J. Stewart, Nano Lett. **1**, 277 (2001) doi:10.1021/nl0155375

S.G. Moorjani, L. Jia, T.N. Jackson, W.O. Hancock, Nano Lett. **3**, 633 (2003) doi:10.1021/nl034001b

C. Reuther, L. Hajdo, R. Tucker, A.A. Kasprzak, S. Diez, Nano Lett. **6**, 2177 (2006) doi:10.1021/nl0609221

W.M. Saxton, M.E. Porter, S.A. Cohn, J.M. Scholey, E.C. Raff, J.R. Mcintosh, Proc. Natl. Acad. Sci. USA **85**, 1109 (1988) doi:10.1073/pnas.85.4.1109

K. Svoboda, C.F. Schmidt, B.J. Schnapp, S.M. Block, Nature **365**, 721 (1993) doi:10.1038/365721a0

R.D. Vale, R.J. Fletterick, Annu. Rev. Cell Dev. Biol **13**, 745 (1997) doi:10.1146/annurev.cellbio.13.1.745

V. VanBuren, L. Cassimeris, D.J. Odde, Biophys. J. **89**, 2911 (2005) doi:10.1529/biophysj.105.060913

V. Verma, W. O. Hancock, J. M. Catchmark, *Advanced Packaging, IEEE Transactions on [see also Components, Packaging and Manufacturing Technology, Part B: Advanced Packaging, IEEE Transactions on]*, **28**, 584 (2005)

C. Vieu, F. Carcenac, A. Pepin, Y. Chen, M. Mejias, A. Lebib et al., Appl. Surf. Sci. **164**, 111 (2000) doi:10.1016/S0169-4332(00)00352-4

F.D. Warner, J.R. McIntosh, *Cell movement, Volume 2, kinesin, dynein and microtubule dynamics*, 431–440. Pages Liss, New York (1999)

R.C. Williams Jr., J.C. Lee, Methods Enzymol Pt B **85**, 376 (1982)

A.P. Yong Chen, Electrophoresis **22**, 187 (2001) doi:10.1002/1522-2683(200101)22:2<187::AID-ELPS187>3.0.CO;2-0